

10 GHz femtosecond pulse interleaver in planar waveguide technology

Michelle Y. Sander,^{1*} Sergey Frolov,² Joseph Shmulovich,² Erich P. Ippen,¹
and Franz X. Kärtner^{1,3}

¹Department of Electrical Engineering and Computer Science and Research Laboratory of Electronics,
Massachusetts Institute of Technology, 77 Massachusetts Avenue, Cambridge, MA 02139, USA

²CyOptics, Inc., South Plainfield, NJ 07080, USA

³Center for Free-Electron Laser Science, Deutsches Elektronen-Synchrotron and Universität Hamburg,
Notkestraße 85, D-22607 Hamburg, Germany

*sander@mit.edu

Abstract: Coherent pulse interleaving implemented in planar waveguide technology is presented as a compact and robust solution to generate high repetition rate frequency combs. We demonstrate a 10 GHz pulse train from an Er-doped femtosecond fiber laser that is coupled into waveguide interleavers and multiplied in repetition rate by a factor of 16. With thermal tuning of the chip elements, we achieve optical and RF sidemode suppression levels of at least -30 dB.

©2012 Optical Society of America

OCIS codes: (320.7090) Ultrafast lasers; (320.7160) Ultrafast technology; (230.3120) Integrated optics devices; (130.2755) Glass waveguides.

References and links

1. E. Ippen, A. Benedick, J. Birge, H. Byun, L. Chen, G. Chang, D. Chao, J. Morse, A. Motamedi, M. Sander, G. Petrich, L. Kolodziejski, and F. Kärtner, "Optical arbitrary waveform generation," in *Conference on Lasers and Electro-Optics (CLEO), 2010, JThC4* (2010).
2. S. T. Cundiff, "Metrology: new generation of combs," *Nature* **450**(7173), 1175–1176 (2007).
3. M. T. Murphy, T. Udem, R. Holzwarth, A. Sismann, L. Pasquini, C. Araujo-Hauck, H. Dekker, S. D'Odorico, M. Fischer, T. W. Hänsch, and A. Manescau, "High-precision wavelength calibration of astronomical spectrographs with laser frequency combs," *Mon. Not. R. Astron. Soc.* **380**(2), 839–847 (2007).
4. C. H. Li, A. J. Benedick, P. Fendel, A. G. Glenday, F. X. Kärtner, D. F. Phillips, D. Sasselov, A. Szentgyorgyi, and R. L. Walsworth, "A laser frequency comb that enables radial velocity measurements with a precision of 1 cm s^{-1} ," *Nature* **452**(7187), 610–612 (2008).
5. T. Steinmetz, T. Wilken, C. Araujo-Hauck, R. Holzwarth, T. W. Hänsch, L. Pasquini, A. Manescau, S. D'Odorico, M. T. Murphy, T. Kentscher, W. Schmidt, and T. Udem, "Laser frequency combs for astronomical observations," *Science* **321**(5894), 1335–1337 (2008).
6. A. Bartels, S. A. Diddams, C. W. Oates, G. Wilpers, J. C. Bergquist, W. H. Oskay, and L. Hollberg, "Femtosecond-laser-based synthesis of ultrastable microwave signals from optical frequency references," *Opt. Lett.* **30**(6), 667–669 (2005).
7. J. Millo, R. Boudot, M. Lours, P. Y. Bourgeois, A. N. Luiten, Y. Le Coq, Y. Kersalé, and G. Santarelli, "Ultra-low-noise microwave extraction from fiber-based optical frequency comb," *Opt. Lett.* **34**(23), 3707–3709 (2009).
8. F. Quinlan, T. M. Fortier, M. S. Kirchner, J. A. Taylor, M. J. Thorpe, N. Lemke, A. D. Ludlow, Y. Jiang, and S. A. Diddams, "Ultralow phase noise microwave generation with an Er: fiber-based optical frequency divider," *Opt. Lett.* **36**(16), 3260–3262 (2011).
9. S. A. Diddams, M. Kirchner, T. Fortier, D. Braje, A. M. Weiner, and L. Hollberg, "Improved signal-to-noise ratio of 10 GHz microwave signals generated with a mode-filtered femtosecond laser frequency comb," *Opt. Express* **17**(5), 3331–3340 (2009).
10. M. Kuznetsov, "Cascaded coupler Mach-Zehnder channel dropping filters for wavelength-division-multiplexed optical systems," *J. Lightwave Technol.* **12**(2), 226–230 (1994).
11. X. Liu, C. Yu, Z. Zeng, and L. Liu, "Design and applications of planar waveguide interleaving filters," *Proc. SPIE* **5623**, 594–604 (2005).
12. M. Oguma, T. Kitoh, Y. Inoue, T. Mizuno, T. Shibata, M. Kohtoku, and Y. Hibino, "Compact and low-loss interleave filter employing lattice-form structure and silica-based waveguide," *J. Lightwave Technol.* **22**(3), 895–902 (2004).
13. T. Chiba, "Waveguide interleaving filters," *Proc. SPIE* **5246**, 532–538 (2003).
14. S. Cao, J. Chen, J. Damask, C. Doerr, L. Guiziou, G. Harvey, Y. Hibino, H. Li, S. Suzuki, K. Wu, and P. Xie, "Interleaver technology: comparisons and applications requirements," *J. Lightwave Technol.* **22**(1), 281–289 (2004).

15. M. Kawachi, "Silica waveguides on silicon and their application to integrated-optic components," *Opt. Quantum Electron.* **22**(5), 391–416 (1990).
16. H. G. Weber and M. Nagazawa, *Ultra-high-Speed Optical Transmission Technology* (Springer, 2007).
17. P. Guan, T. Hirano, K. Harako, Y. Tomoyama, T. Hirooka, and M. Nagazawa, "2.56 Tbit/s/ch polarization-multiplexed DQPSK transmission over 300 km using time-domain optical Fourier transformation," in *ECOC Technical Digest*, 2011, We.10.P1.80 (2011).
18. H. Byun, D. Pudo, S. Frolov, A. Hanjani, J. Shmulovich, E. P. Ippen, and F. X. Kärtner, "Integrated 2 GHz femtosecond laser based on a planar Er-doped lightwave circuit," in *Conference on Lasers and Electro-Optics (CLEO), 2010*, CFE5 (2010).
19. M. Y. Sander, H. Byun, J. Morse, D. Chao, H. M. Shen, A. Motamedi, G. Petrich, L. Kolodziejski, E. P. Ippen, and F. X. Kärtner, "1 GHz femtosecond erbium-doped fiber lasers," in *Conference on Lasers and Electro-Optics (CLEO), 2010*, CTu11 (2010).
20. H. Byun, M. Y. Sander, A. Motamedi, H. Shen, G. S. Petrich, L. A. Kolodziejski, E. P. Ippen, and F. X. Kärtner, "Compact, stable 1 GHz femtosecond Er-doped fiber lasers," *Appl. Opt.* **49**(29), 5577–5582 (2010).
21. M. Y. Sander, H. Byun, M. Dahlem, D. Chao, A. R. Motamedi, G. Petrich, L. Kolodziejski, S. Frolov, H. Hao, J. Shmulovich, E. P. Ippen, and F. X. Kaertner, "10 GHz waveguide interleaved femtosecond pulse train," in *Conference on Lasers and Electro-Optics (CLEO), 2011*, CThY6 (2011).
22. S. Cundiff, B. Collings, and W. Knox, "Polarization locking in an isotropic, modelocked soliton Er/Yb fiber laser," *Opt. Express* **1**(1), 12–21 (1997).

1. Introduction

Frequency combs have become an enabling technology for a vast range of applications. Combs with wide frequency spacing - at repetition rates of 10 GHz or higher - exhibit the advantage that their individual frequency lines can be accessed with current filter and modulator technology to efficiently shape the frequency spectrum. Thus, high repetition rate femtosecond oscillators are attractive for optical arbitrary waveform generation [1], high-resolution sampling and frequency metrology [2]. Furthermore, frequency combs have successfully opened a pathway to improve the calibration accuracy of astronomical spectrographs [3–5]: To explore extra-solar planets, changes in the radial velocity in the presence of planets are detected as Doppler shifted starlight. These shifts are measured and compared to a reference source spanning a wide bandwidth from the visible to the near IR. By utilizing frequency combs with their inherent high wavelength accuracy and long-term stability, the calibration resolution can be significantly enhanced. For the frequency comb to efficiently match the resolving power of spectrographs, comb spacings of 10 GHz or higher are required. Currently, fundamental frequency combs at lower repetition rates are therefore externally filtered with Fabry-Perot cavities to obtain the desired multi GHz spacing and to suppress the extraneous comb lines by ~25 dB [4,5]. However, any non-uniform intensity distribution, like asymmetric amplitudes of the filtered sidemodes in the frequency comb, gets enhanced in any nonlinear broadening process to obtain a wide-band frequency comb. This leads to a center of gravity frequency shift that can result in systematic wavelength offsets, limiting the detection resolution and distorting the absolute stellar radial velocity values. Therefore, a long-term stable, wide-spaced frequency source with high wavelength accuracy and good sidemode suppression is essential to identify planets beyond the resolving range of current state-of-the-art spectrographs.

Optical frequency combs can also be utilized to generate low-noise microwave signals through optical frequency division [6–8]. By detecting the optical pulses with a wide-bandwidth photodiode, an electric pulse train is generated consisting of single tones at the laser repetition rate and its harmonics up to the cut-off frequency of the detector. The phase-coherence of the optical lines enables a RF signal train with good stability, low noise and high spectral purity. After subsequent filtering of the desired RF frequency line, the obtained microwave source can outperform current state-of-the-art low-phase microwave oscillators. Diddams et al. [9] demonstrated an improvement in the shot-noise-limited signal-to-noise performance of higher harmonic microwave signals by external optical filtering with a Fabry-Perot cavity before detection on the photodiode. Thus, for the filtered 10 GHz signal, 10 dB signal strength could be gained compared to the 10th harmonic of the fundamental 1 GHz source. Instead of a Fabry-Perot cavity to filter the signal, which requires a high finesse for sharp transmission peaks, interleavers based on Mach-Zehnder interferometers present an elegant alternative. These interleavers can be implemented in planar waveguide circuits with

a small and compact footprint. As such, they have distinct advantages over free-space, alignment sensitive set-ups like Fabry-Perot cavities, offering long-term reliability, robustness and easy portability.

Interleaver filters based on planar waveguide technology have consistently evolved over the years, in particular for dense wavelength division multiplexed optical fiber systems. To satisfy the growing demand for more information capacity, fiber coupled and planar waveguide optical interleavers have been utilized to increase the channel spacing. These interleaving filters were primarily designed for wide-bandwidth pass-bands by cascading multiple stages and optimizing the coupling coefficient ratios at each individual interleaver stage for operating frequencies around 50-100 GHz [10–13]. A good overview over different interleaver implementations can be found in Cao [14] and Kawachi [15], who outlines the various silica waveguide technology components. Waveguide interleavers can be directly coupled to existing fiber platforms or integrated in the same fabrication process with emerging silicon photonics, thus providing a compact solution with robust performance metrics. In addition, the waveguide chip fabrication is scalable. For this work, we combine interleavers with thermal phase shifters to explore coherent pulse interleaving. By cascading several interleaver stages, higher multiples of the initial repetition rate are achieved.

To realize optical time division multiplexing systems with transmission speeds above 1 Tbit/s, femtosecond pulses are used in combination with different fiber based techniques [16]. Recently, Nakazawa demonstrated a 32-times interleaved femtosecond pulse for 2.56 Tbit/s/ch polarization multiplexed transmission with reduced polarization-mode dispersion impairments in a differential quadrature phase-shift keying configuration [17]. However, to the best of our knowledge, planar waveguide interleavers for coherent pulse interleaving of femtosecond pulses have not been extensively explored in literature so far. We have previously reported an integrated waveguide system consisting of a 500 MHz waveguide laser combined with a two-stage interleaver to produce a 2 GHz fs-pulse output train [18]. However, the maximum RF sidemode suppression was limited to 15 dB due to fabrication tolerances in the coupling ratios.

In the following, we present a hybrid system of an Er-doped fiber laser combined with silica waveguide interleavers. The goal of this research is to demonstrate that an integrated waveguide device can be utilized for coherent pulse interleaving around 1550 nm and for scaling the repetition rate to 10 GHz. The interleavers are designed specifically to incorporate a thermal tuning mechanism, so that fabrication tolerances can be compensated, which otherwise limit the sidemode suppression. We show that this combination of recent progress in mode-locked fiber lasers [19–21] with waveguide interleavers enables us to scale the repetition rate of a fundamentally mode-locked femtosecond laser reliably by a factor of 16 with a good sidemode suppression of at least 30 dB. At the same time, we demonstrate a compact footprint and robust system to obtain a 10 GHz coherent pulse train. The following results underline the promising potential of this technology for various applications in science and engineering.

2. Interleaver design and set-up

Waveguide interleavers were designed for an implementation in planar waveguide technology as illustrated in Fig. 1(a): In each interleaver stage, the input signal is divided by a directional coupler into two pulse trains, one of which experiences a differential delay $\tau_1 = 1/(2f_{rep})$ of half the initial pulse train spacing $1/f_{rep}$, before both waveguide arms are re-combined. By incorporating two interleavers with respective delay line lengths of $d_1 = c/(n \cdot \tau_1)$ and $d_2 = d_1/2$ (with c the speed of light and n the refractive index) on one interleaver chip, the input repetition rate is quadrupled. This first interleaver chip, consisting of a 2-stage interleaver, is cascaded with a second interleaver chip featuring another 2-stage interleaver with respective delay line lengths of $d_1/4$ and $d_1/8$. Thus, in four interleaver stages on two chips, the repetition rate is multiplied overall by a factor of 16.

To obtain a phase-coherent output pulse, the repetition rate and filter spacing have to be matched and the absolute positions of the frequency lines have to coincide with the filter

notches. Thus, for coherent pulse interleaving with a good sidemode suppression ratio, it is crucial that the delay line lengths are matched to the input repetition rate f_{rep} . This is achieved by implementing post-fabrication tuning mechanisms to compensate for any fabrication tolerances. Thermal heaters were incorporated on top of each interleaver arm for tuning of the delay lines to the desired length. In addition, the directional couplers are fabrication sensitive since the coupling efficiency depends on the effective coupler length and the gap between the two waveguide arms. To obtain exact phase delays and an overall 50/50 splitting ratio in the directional couplers, an additional coupler with a thermally tunable waveguide section $L \approx 2$ mm was included for each Mach-Zehnder interferometer stage. The induced relative phase-shifts by thermal tuning of the heaters in these Mach-Zehnder interferometers with up to 50 mW applied heater power, counterbalanced nominal deviations of $\pm 5\%$ from 50% in the coupling ratio.

As host material, passive Ge-doped $4 \mu\text{m} \times 4 \mu\text{m}$ silica waveguides with a $10 \mu\text{m}$ silicon oxide cladding on a silicon substrate were selected for low loss and low dispersion waveguides around 1550 nm. The high index contrast of 1.5% enabled tighter bending radii for the waveguides without introducing significant mode losses. A folded design layout was pursued to obtain a compact chip, in particular of interest for the interleaver stages with longer delay lines ($d_l = 16$ cm for the first interleaver stage from 625 MHz to 1.25 GHz). Two interleaver stages were integrated on each chip with a footprint of $19.4 \text{ mm} \times 10.5 \text{ mm}$. Two different interleaver chips, resulting in a 4-stage interleaver, were fabricated to overall multiply the repetition rate by a factor of 16 from 625 MHz to 10 GHz. To minimize coupling losses to a permanently attached fiber array with regular SMF-28e fiber, mode-converters adjusted the mode size through waveguide tapering. The heater connection pads were wire-bonded to a printed circuit board so that each heater could be individually controlled through a digital-to-analog converter board.

A soliton mode-locked fiber laser served as input source to the waveguide interleaver chip, see Fig. 1(b). The linear fiber laser cavity consisted of 12.5 cm long Er-doped gain fiber (Liekki Er80-8/125 with anomalous dispersion of $-20 \text{ fs}^2/\text{mm}$) that was imaged onto an in-house fabricated semiconductor saturable Bragg reflector (SBR) [19–21]. A thin-film polarizer in the free-space section served as a polarization discriminating element to ensure a constant output polarization and to suppress periodic polarization rotation of vector solitons [22]. The modular approach with an Er-doped fiber laser source provided the distinct advantage that the repetition rate, input polarization and pulse duration could be adjusted and matched to the interleaver filters. The pulse was amplified in two isolated stages of Er-doped amplifiers, which were optimized in their design for maximum gain and minimum amplified spontaneous emission contribution. The amplifiers incorporated Er-doped normal dispersion gain sections (Liekki Er110-4/125). They were pumped in a counter-propagating scheme with launched pump powers of 500 mW and 400 mW. With an external fiber polarization control unit, the input polarization into each interleaver chip was optimized to the preferred waveguide mode. The free-space section in the fiber laser cavity allowed tuning the laser repetition rate around 625 MHz, so that the laser frequency lines could be matched to the interleaver filter response and the device performance could be optimized. Further fine-adjustments to the optical transmission function were made afterwards by thermal tuning of the delay lines.

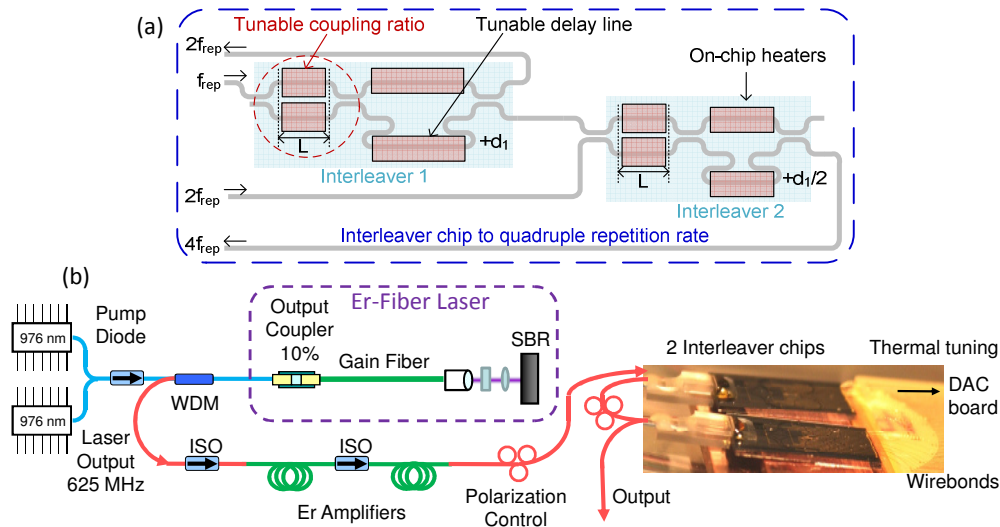


Fig. 1. (a) Schematic of a 2-stage interleaver where each interleaver stage consists of a tunable Mach-Zehnder interferometer to adjust the coupling ratio in the directional couplers and a thermally tunable delay line. Each interleaver chip comprises two interleaver stages to quadruple the input repetition rate. By cascading two interleaver chips with the respective delay line lengths to obtain a 4-stage interleaver, a total multiplication by a factor of 16 of the repetition rate can be achieved. (b) Experimental set-up: A saturable Bragg reflector (SBR) mode-locked 625 MHz Er-doped fiber laser is pumped by two polarization combined semiconductor pump diodes through a wavelength division multiplexer (WDM) [19]. The output is amplified in two isolated (isolator ISO) stages before it is coupled into two cascaded waveguide interleaver chips.

3. Characterization

3.1 Optical spectrum results

The Er-doped fiber laser was stably mode-locked at a fundamental repetition rate of 624.5 MHz. An output power of 4.6 mW was obtained for 420 mW of launched pump power from two polarization combined pump diodes. The optical spectrum of the Er-doped fiber laser, shown in Fig. 2(a), featured a 3-dB full-width half-maximum (FWHM) bandwidth of 6.1 nm. Assuming soliton propagation in form of sech-shaped pulses, this optical bandwidth corresponds to 420 fs transform limited pulses. The laser output, after passing a 1550 nm isolator, was amplified in two isolated Er-doped amplifier stages from 3 mW to 82 mW before being coupled into the waveguide chips. In both amplifiers, gain narrowing and spectral shaping due to nonlinearities and self-phase modulation could be observed. This resulted in additional spectral side-lobes as seen in Fig. 2(a) (dotted gray line). The second amplifier stage limited the optical bandwidth further, so that the output spectrum of the interleaver featured only a 4 nm 3-dB bandwidth, cf. Fig. 2(a) (red line). Nonetheless, pre-amplification was favorable to post-amplification of the interleaver output pulse train; otherwise the sideband suppression got distorted due to four-wave mixing and nonlinear amplification. The optical modes with a spacing of ~ 0.08 nm in the interleaver output spectrum, as illustrated in Fig. 2(b), show only limited contrast due to the 0.1 nm resolution of the optical spectrum analyzer used. Though not fully resolved, these optical modes confirmed the phase-coherence of the 10 GHz output pulse train. The time-domain oscilloscope traces of the laser output in Fig. 2(c) and the 2-stage interleaver output at 2.5 GHz in Fig. 2(d) demonstrate the good signal stability. The pre- and post-pulses in Fig. 2(d) can be explained by detector ringing and ghost images were likely caused by cable artefacts.

The Ge-doped silica waveguides were low-loss with around 0.01 dB/cm, resulting in propagation losses of 0.3 dB for the longest arm in the 4-stage interleaver. Interleaver losses

of 3 dB due to power division into two arms were encountered in every stage, resulting in a 12 dB loss for a 4-stage interleaver. With standard coupling losses of 1.5 dB between the chip and fiber array, theoretically expected losses for the overall waveguide system amounted to approximately 18 dB. However, the 10 GHz interleaver output signal with 150 μ W of output power (for 82 mW input power), indicated significant additional excess losses in the interleaver system, featuring up to 27 dB of total losses. Optical time domain reflectometry measurements established the occurrence of high front-end reflections. Thus, these high excess losses of 9 dB were partially attributed to high input facet and surface scattering losses, polarization coupling losses, and inherent waveguide losses for pulsed operation in this initial waveguide fabrication run.

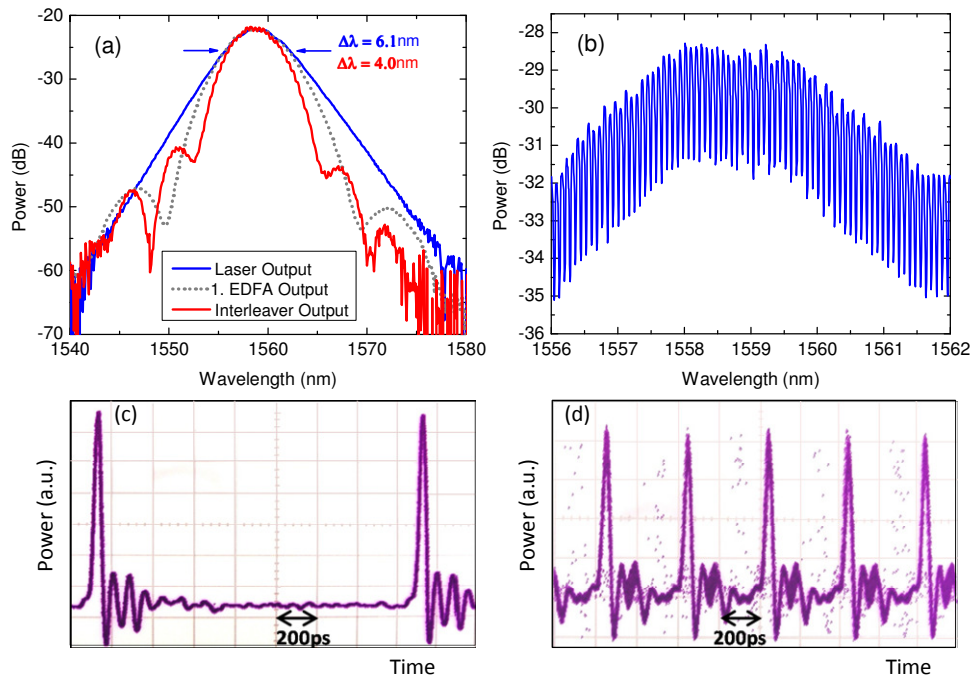


Fig. 2. (a) Optical spectrum of laser output with 6.1 nm 3-dB bandwidth (blue line); output after first Er-doped fiber amplifier (EDFA) (dotted grey line) and 10 GHz interleaver output with 4 nm FWHM bandwidth (red line). (b) Optical spectrum of the 4-stage interleaver output, optical modes corresponding to 10 GHz line spacing barely resolved by the 0.1 nm resolution of the optical spectrum analyzer used. (c) Time-domain oscilloscope trace of the laser output, pulse train spacing corresponding to \sim 625 MHz repetition rate. (d) Time-domain oscilloscope trace of the 2-stage interleaver output at 2.5 GHz.

3.2 Optical transmission

To characterize the interleaver chips and their performance independently from the fiber laser pulses, the optical transmission of each individual interleaver stage was measured with a tunable, continuous wave (cw) laser. That way, the linear chip losses and the expected suppression levels could be determined: A tunable, high precision laser source (TLS, Agilent 81640A, 2 mW output power) was swept with 0.1 pm step size resolution over different wavelength ranges. For each measurement, the input polarization of the TLS into the interleaver and the thermal tuning state were adjusted. In the following, results centered at 1560 nm are presented. For the first interleaver stage from 625 MHz to 1.25 GHz (corresponding to 10 pm wavelength spacing for the free spectral range), the measured maximum suppression for the optical transmission indicated a value of at least 27.3 dB with thermal tuning, cf. Fig. 3(a). However, these results were highly polarization sensitive and

depended explicitly on the applied heater power due to additionally introduced waveguide birefringence and subsequent polarization conversion with thermal tuning. Given the different degrees of freedom in the system, it proved challenging to optimize the input polarization sufficiently at the filter minima (down to -35 dBm) so that only one waveguide polarization was guided. Thus, by monitoring the power for one input wavelength, only states close to a local minimum could be found. Simulation of the transmission characteristics indicated that even with small deviations in the coupling ratio, overall better optical suppression should be obtainable. At the same time, we inferred from the modeling that a source resolution and stability of better than 0.2 pm was required to measure optical suppression levels better than 30 dB for the first interleaver stage, which featured the narrowest dips compared to the other interleaver stages. Therefore, the actual depth of the notches in the optical transmission was most likely not fully detected due to TLS wavelength jitter and superimposed polarization states. Figure 3(b) depicts the optical transmission for two interleaver stages without thermal tuning. Maximum suppression levels of 34.2 dB were recorded. In this particular state, the maximum optical suppression obtained from the first interleaver was measured to be 21.8 dB. In addition, the measurement confirmed high excess losses, also in cw operation, for the waveguide chips.

Modeling the optical transmission for the 2-stage interleaver system and optimizing the different coupling coefficients to match the experimental results, we concluded that, without any thermal tuning, fabrication tolerances caused deviations from the ideal 50%-50% splitting ratio by ± 2 -3% (consistent with $\pm 5\%$ expected variations). Figure 3(c) shows the simulated transmission with ± 2 -3% offsets in the coupling coefficients as a continuous blue curve with maximum suppression levels similar to the measured values shown in Fig. 3(b). To relate the transmission curves to the expected optical suppression for a femtosecond pulse train, red dots in Fig. 3(c) mark the optical suppression for frequency lines at multiples of the repetition rate. Over the displayed wavelength range of 80 pm, corresponding to 10 GHz, the waveguide dispersion (measured anomalous dispersion with -5 fs²/mm) shifted the optical transmission curve slightly towards longer wavelengths: The time delay accumulated in the delay lines got modified by group delay dispersion. Thus, over a given wavelength interval, a walk-off between the frequency lines and the minima in the transmission curve occurred, as visible in Fig. 3(c). Additionally, fabrication tolerances in the delay lines enhanced this effect. In this instance, deviations in the delay line lengths were assumed to be fairly small, on the order of $0.0025 \cdot \lambda = 3.9$ nm. Due to anomalous dispersion, the fabrication length offsets could partially be compensated for by reducing the repetition rate. However, over a large bandwidth the filter notches and frequency lines eventually became significantly misaligned. This is shown in Fig. 3(d) where for the first interleaver stage the maximum and minimum values at harmonics of the repetition rate (at 623 MHz) are plotted. The decreasing sidemode suppression due to the delay line length tolerances and group delay of the pulses accumulated in the longer waveguide arm is clearly visible. This process is periodic in wavelength and in this particular case a good suppression was reached again within an 8 nm interval.

While the impact of group delay can be clearly detected in the frequency domain, temporal broadening due to group velocity dispersion of the pulse itself can be neglected. For a FWHM pulse duration of 420 fs, the total accumulated dispersion in the 4-stage interleaver system amounts to -1500 fs² (based on the measured waveguide dispersion of -5 fs²/mm), corresponding to a negligible total dispersive phase shift of ~ 0.02 rad. Theoretical modeling confirmed that no significant pulse stretching occurs ($< 0.5\%$ in pulse duration). Moreover, for the considered frequency comb applications, the absolute pulse duration itself is only of secondary nature as long as the desired spectral bandwidth is covered.

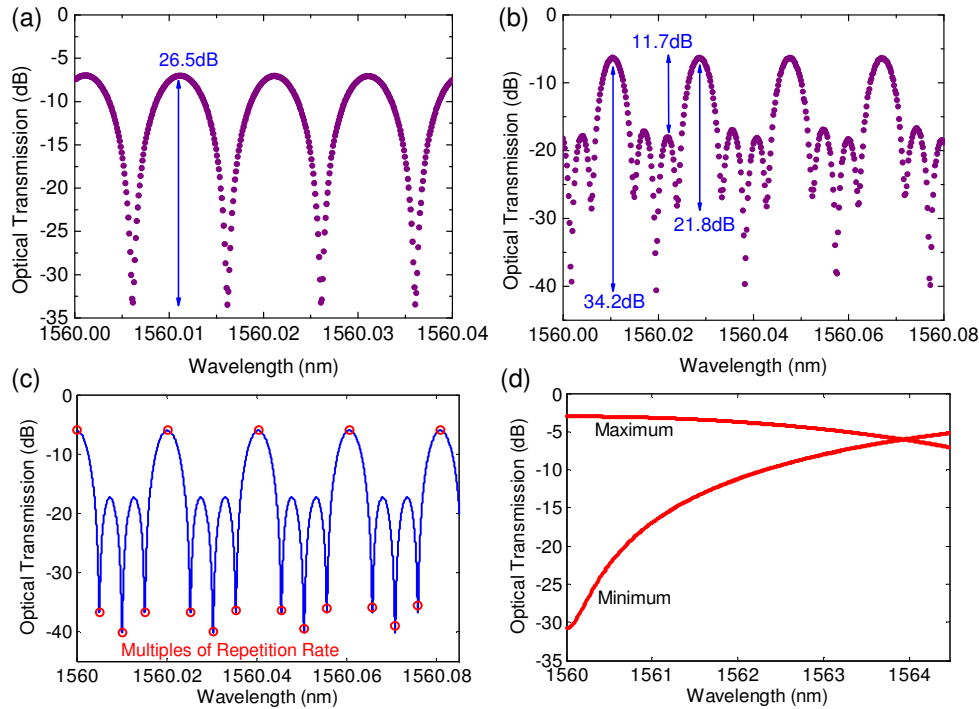


Fig. 3. Optical transmission measurements of (a) first interleave stage at 1.25 GHz with thermal tuning and (b) cascaded first two interleave stages at 2.5 GHz. (c) Simulated optical transmission (blue line) for 2.5 GHz interleave output. Optical suppression of frequencies at multiples of the repetition rate of 624 MHz are marked by red dots. (d) Waveguide dispersion (of $-5 \text{ fs}^2/\text{mm}$) limits the modeled optical suppression as the evolution of maximum and minimum at harmonics of the repetition rate at 623 MHz are plotted for one interleave stage.

3.3 RF characterization

The RF spectrum measurement provided an evaluation of the combined fiber and interleave system, whose performance metrics are of interest for low-noise microwave generation. The RF data, as illustrated in Fig. 4, were taken for a fundamental repetition rate of the fiber laser at 624.5 MHz, where the suppression was found to have been maximized. The RF-domain interleave output at 2.5 GHz is presented in Fig. 4(a) and Fig. 4(b). Without thermal tuning, the sub-harmonics were suppressed in the RF domain by 14.3 dB for the immediately adjacent sidebands while the maximum suppression amounted to 22.4 dB. Significant improvement was achieved by thermal tuning as presented in Fig. 4(b): The maximum suppression increased to 55.8 dB for one line, where the interleave response and input frequency directly lined up in a transmission minimum. Over the frequency span up to 12 GHz, the minimum sidemode suppression amounted to at least 30.5 dB. In the thermally tuned state, the sidemode suppression decreased with higher harmonics. This can partially be explained by the limiting impact of wavelength dependent coupling coefficient offsets and waveguide dispersion. As the RF signal is the sum of all convoluted frequency lines, wavelengths at the edges of the optical spectrum can increase the amplitude, since the suppression is not as optimized in those regions. The 2.5 GHz pulse train was then transmitted through the second interleave chip which multiplied the repetition rate to 10 GHz. The initial minimum RF suppression around 15.4 dB for the adjacent sidemode, as shown in Fig. 4(c), was significantly enhanced in the thermally tuned system, as demonstrated in Fig. 4(d). Here, a minimum sideband suppression of 31.3 dB was recorded. Due to the low output power obtained from the interleave chips, the maximum sidemode suppression of 36.3

dB was limited by the detector noise floor. Therefore, it is possible that the actual maximum suppression was greater than the measured value. For these measurements the RF suppression was maximized by tuning of the heaters that primarily adjust the coupling ratio. Thermal tuning of the delay lines mostly influenced the optical suppression of each individual line, as discussed in the following section.

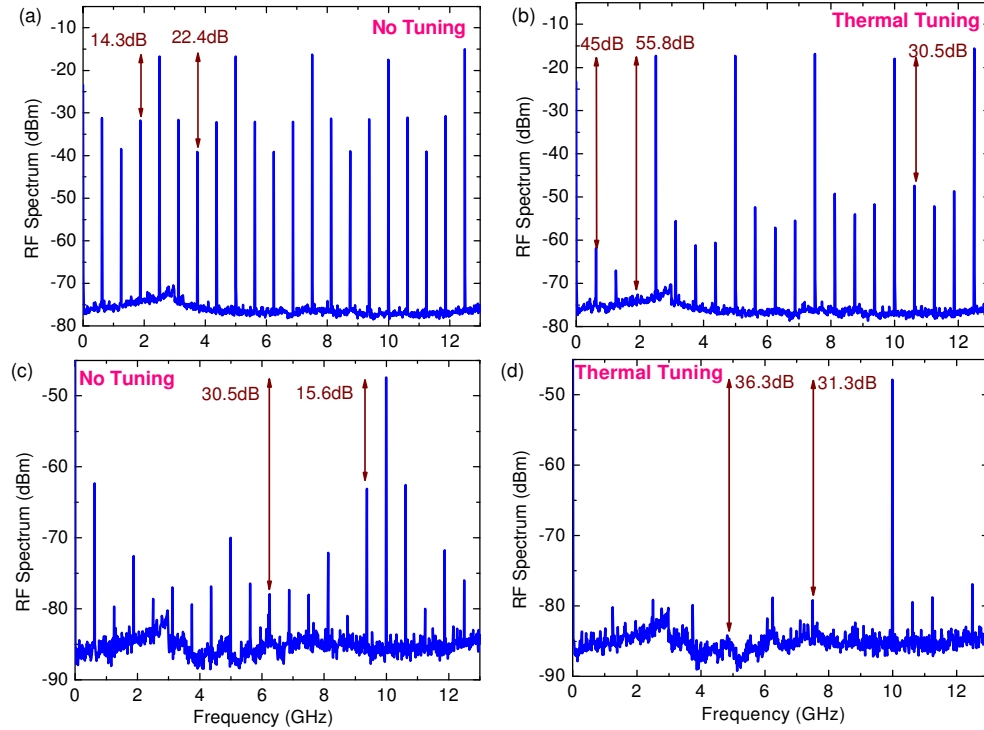


Fig. 4. RF Spectrum: (a) Minimum suppression of 14.3 dB for 2.5 GHz output without thermal tuning. (b) Minimum suppression of 30.5 dB for 2.5 GHz output with thermal tuning. (c) Minimum suppression of 15.6 dB for 10 GHz output without thermal tuning. (d) Minimum suppression of 31.3 dB for 10 GHz output with thermal tuning. All measurements were recorded with a resolution bandwidth of 300 kHz.

3.4 Optical heterodyne beat measurements

To confirm the phase-coherence of the interleaved pulses and to gain insight into the achievable optical suppression, optical heterodyne beat measurements between the interleaved pulse train and a narrow-linewidth tunable laser source were performed.

An optical heterodyne system, as shown in Fig. 5(a), was employed to determine the optical suppression for the individual optical modes in a frequency comb, in particular of interest for frequency metrology applications: The interleaver output was combined with a single frequency narrow-bandwidth line of a stable tunable laser whose polarization was matched to the interleaver output with an external polarization control unit. The signal was recorded by a photo-detector InGaAs EOT ET-3500F. An electronic signal analyzer was the preferred instrument of choice (over a RF power meter) to not only record the amplitude but also the frequency position of the beat notes.

The measured heterodyne optical beat is determined by the respective electric field strengths of the tunable laser source E_{TLS} and the interleaver $E_{\text{TLS}} \cdot E_{\text{Int}}$. Thus, the detected beat note in the RF spectrum analyzer is proportional to the optical interleaver power and the measured suppression corresponds directly to the optical suppression. As the cw transmission

plots described in Section 3.2 record the transmitted optical power through the interleaver device, both measurements provide an independent evaluation of the optical suppression.

To detect the heterodyne beat note, two variations of the measurement set-up were pursued. In the first configuration, the photo-detected signal was low-pass filtered with a cut-off frequency at 450 MHz, as illustrated in the schematic in Fig. 5(a). During each measurement, the beat notes with two neighbouring optical lines were captured, if the TLS line was positioned accordingly. For the first interleaver stage, shown in Fig. 5(b), we found that the optical suppression featured a minimum value of 31 dB at 1560 nm. However, even though the measurement sensitivity of the instrument was optimized to the signal input power, the lower optical beat note disappeared in the noise floor. To obtain the optical suppression for subsequent lines and to examine two or more cascaded interleavers, multiple measurements were made while the tunable laser wavelength source was swept over the desired wavelength range. In Fig. 5(c), three such optical heterodyne measurements for two cascaded interleaver stages were superimposed. The measurements were each taken with 5 pm spacing (corresponding to the initial 624.5 MHz repetition rate) so that neighbouring lines were resolved. The best suppression measured 34.2 dB for the immediate adjacent sidemode, whereas the other two optical lines were suppressed by 22.5 dB. By choosing these wavelength spacings, the optical heterodyne beat corresponding to the previous measurement was recorded again. As identical amplitudes for the same beat note were detected, the consistency of the measurements was confirmed over the recorded interval. However, due to the number of measurements required, this method is only suitable for an interleaver analysis with few stages.

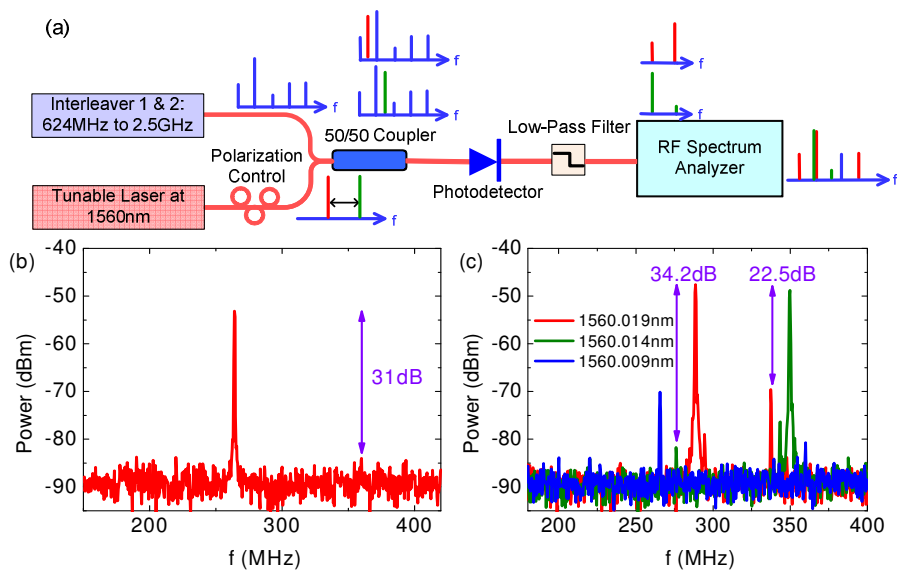


Fig. 5. (a) Measurement set-up to detect the optical heterodyne beat for two cascaded interleaver stages. Different colors (red, green) indicate two different wavelengths of the tunable laser. (b) Minimum optical suppression of 31 dB at 1560 nm for 1.25 GHz interleaver. (c) Maximum optical suppression of 34.2 dB around 1560 nm for 2.5 GHz interleaver. Three measurements at different wavelengths are combined in one plot to obtain information about the suppression over one free spectral range. All measurements featured a resolution bandwidth of 300 kHz.

To maximize the optical suppression information obtained within one measurement, a second measurement configuration with a wide-band frequency approach (without the low-pass filter in Fig. 5(a)) was pursued. In this set-up, the beat notes between the single wavelength laser and all optical interleaver lines were detected simultaneously. Results for the 2-stage interleaver at 2.5 GHz are shown in Fig. 6. Here, the minimum suppression ratio

varied between 25.2 dB and 29.9 dB. In this particular state, the system was optimized by tuning the coupler and delay line heaters for a symmetric suppression of the sidemodes. This more uniform power distribution obtained is in particular attractive for astrocomb calibrations. During each measurement the harmonics of the repetition rate lines (plotted in grey in Fig. 6) were detected together with the optical heterodyne beats (highlighted in red). As the repetition rate signal and its harmonics were given by a convolution of all optical lines, they possessed significantly more power (up to 25 dBm). Thus, the sensitivity towards the low-power optical beat notes had to be reduced for the higher power RF lines not to saturate the detector. This can partially explain the difference in maximum sidemode suppression of 29.9 dB compared to the first measurement result of 34.2 dB. In addition, each state depended highly on the thermal tuning and input polarization. The good optical suppression over the measurement interval indicates that after thermal tuning the delay line lengths were well matched to the frequency comb lines, as otherwise the suppression would have significantly worsened with higher harmonics.

The optical suppression can be evaluated with this measurement for subsequent stages. Repeating this measurement for the whole 10 GHz interleaver stage showed that maximum suppression levels around 31 dB could be obtained for individual lines.

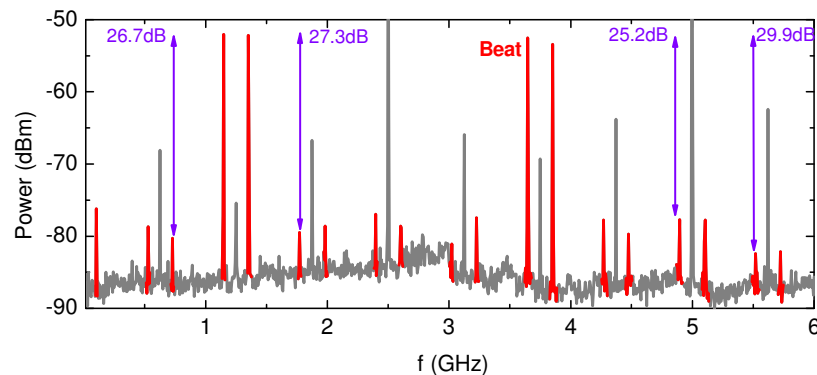


Fig. 6. Heterodyne beat measurement for thermally tuned 2.5 GHz interleaver. The optical beat notes are denoted in red, the grey lines depict multiples of the initial repetition rate.

4. Discussion

Different performance metrics of thermally tunable planar waveguide interleavers were analyzed. The optical transmission measurements confirmed expected device performance and provided insight into how well the fabrication met the target design. It is extremely beneficial to have such a verification that is independent of the fiber oscillator operation and any challenges that come by adding complexity to the system. In addition, these optical suppression values correspond directly to the optical heterodyne beat. While the maximum optical cw transmission suppression for the first interleaver stage amounted to 26.5 dB, the heterodyne beat measurement inferred a value of at least 31 dB. As discussed already in Section 3.2, for the first interleaver stage with narrow minima, the full depth of the notches might not be detected due to the limited wavelength resolution and precision of the TLS. The variation between the two measurements can additionally be explained by different thermally tuned states. For subsequent stages at GHz operating frequencies, the maximum measured optical suppression for the two cascaded interleaver stages from the transmission and heterodyne beat measurement both independently verified corresponding suppression levels, in one case of 34.2 dB, whereas for another operating point the optical suppression was measured to be 29.9 dB. This underlines further how critical the thermal tuning is and how small offsets in the delay lines can affect the optical suppression levels significantly.

The measured harmonics of the repetition rate in the RF spectrum are composed by a convolution of all optical frequency lines in the frequency comb; including the lower power

wings of the spectrum (± 15 nm from 1558 nm) that do not necessarily feature an optimized sidemode suppression. The coupling coefficients deviate more strongly from the ideal splitting ratio in this regime since the directional couplers are wavelength dependent and dispersion can limit the suppression of some individual lines. In addition, phase effects can cancel or enhance certain harmonics of the repetition rate and the delay line lengths might not be matched as well as for the center part of the wavelength spectrum. Therefore, it is crucial to measure the optical and the RF suppression individually.

One limiting factor on the sidemode suppression over a wide bandwidth range was established to be waveguide dispersion and delay line offsets which have to be controlled to within a small fraction of the wavelength. Minimizing waveguide dispersion further or incorporating dispersion compensating designs could reduce this impact. In addition, scaling the fundamental repetition rate of the fiber oscillator to higher repetition rates in the GHz regime allows decreasing the delay length line in the interleaver, which in turn reduces the accumulated dispersion and improves the accuracy of the fabricated delay line length. Furthermore, multiple stages of the same interleaver can be cascaded or the same device double-passed to obtain better overall suppression levels. In addition, current efforts are underway to optimize the interleaver design and the fabrication to reduce the excessive losses in the interleavers. As the excess losses stem mostly from the high front-end reflections of the waveguide interleaver chip, improving the coupling from the fiber array to the chip can reduce the excess losses. Moreover, polarization conversion losses can be minimized by integrating design options to guide only one single polarization.

For a first demonstration of this technology, a free-running fiber laser source was used. Since the laser source was well isolated, the observed repetition rate drifts were below 0.3 kHz over a time span of 10 minutes and fluctuations in the carrier-envelope phase shift were expected to have been even smaller. Therefore, these drifts were not considered to impose limitations on the measurement results. With more optical power available in each line, a fully stabilized laser source and reduced interleaver excess losses, we are optimistic that even better performance metrics can be achieved for generating wide-spaced frequency combs.

5. Conclusion

We demonstrated a compact system of a repetition rate tunable fiber laser combined with four interleaver stages to multiply the repetition rate by a factor of 16, from 625 MHz to 10 GHz. An amplified femtosecond pulse train was coupled from the fiber oscillator source into interleavers defined in planar waveguide geometry. The optical and RF sidemode suppression of the frequency lines was analyzed. The minimum RF suppression of 30 dB up to 12 GHz was found to be partially limited by waveguide dispersion and delay line length offsets. In the optical domain, minimum suppression levels around 30 dB were confirmed by heterodyne beat measurements. Thus, we demonstrated the promising potential of thermally tunable interleavers in planar waveguide geometry for coherent pulse interleaving for applications in astrocomb calibration, frequency metrology and low-noise microwave signal generation.

Acknowledgments

This work was supported in part by the Defense Advanced Research Projects Agency (DARPA) under contract HR0011-05-C-0155 and contract W911NF-04-1-0431, and in part by the Air Force Office of Scientific Research (AFOSR) under contract FA9550-10-1-0063. The authors thank Hyunil Byun for his insightful advice on the fiber laser and interleaver design and Marcus Dahlem for helpful suggestions on the thermal tuning of the interleaver heaters. We are grateful to David Chao for thoughtful discussions and Hong Hao, CyOptics, for sharing his knowledge on attaching fiber arrays to the waveguide chips.